Proceedings of the
Annual Stability Conference
Structural Stability Research Council
Orlando, Florida, April 12-15, 2016

Stability design of columns with intermediate gravity loads

Lip H. Teh[1], Benoit P. Gilbert[2]

Abstract
This paper describes an accurate and economical procedure for determining the flexural effective length of a column subjected to concentrated gravity loads within its unsupported length, for applications in the 2D second-order elastic analysis based design procedure. The presented buckling model has "notional" horizontal restraints where equivalent horizontal forces have been applied, and can be readily programmed into a structural analysis/design software. The performance of the procedure is compared against that using an effective length factor equal to unity and the buckling model described in the European drive-in rack design code. Twenty columns having various end restraint conditions subjected to concentrated gravity loads within their unsupported lengths are analysed to demonstrate the merits of the present procedure. It is demonstrated that, in most of the cases analysed, the present procedure leads to more liberal column capacities compared to the use of the unity effective length factor or the buckling model of the European drive-in rack design code. On average, the more liberal capacities are significantly closer to the ultimate loads determined through second-order plastic-zone analysis.

1. Introduction

This paper is concerned with the stability design of steel columns subjected to concentrated gravity loads within their unsupported lengths. Such columns include mill building columns and drive-in rack uprights. In steel storage rack design standards (ECS 2009, ERF 2012, RMI 2012, SA 2012), the use of equivalent horizontal forces in lieu of explicit modelling of initial out-of-plumb is a well-accepted practice. The equivalent horizontal forces are simply the product of the applied gravity loads and the prescribed initial out-of-plumb, as illustrated in Figure 1, which is adopted from the European adjustable pallet racking code (ECS 2009).

The concept of equivalent horizontal forces is predated by the notional load approach found in the literature (Liew et al. 1994, Clarke & Bridge 1995, ASCE 1997), which aims to capture the initial out-of-plumb (P-Δ), initial crookedness (P-δ), distributed plasticity and residual stress effects on the member forces at the ultimate limit state via the application of notional horizontal loads in a second-order analysis. However, the equivalent horizontal forces in the storage rack design standards principally model the frame's (nominal) initial out-of-plumb only.

[1] Associate Professor, University of Wollongong, <lteh@uow.edu.au>
[2] Senior Lecturer, Griffith University, <b.gilbert@griffith.edu.au>

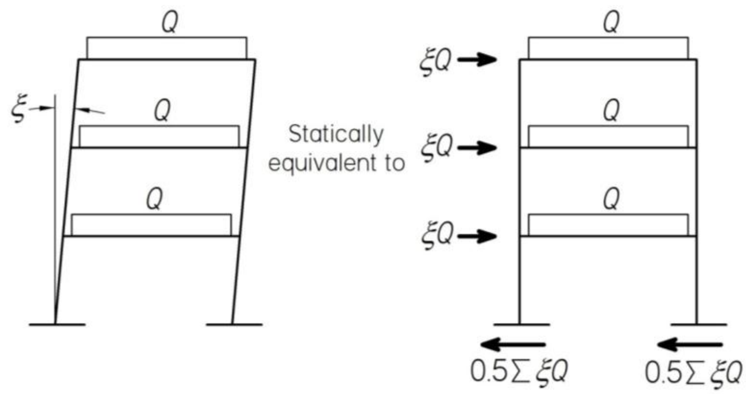

Figure 1 Equivalent horizontal forces (ECS 2009)

The notional load approach has been promoted as a method that enables the use of the "actual unsupported length" of a column in its stability design check. However, in contrast to regular rectangular frames (White & Clarke 1997, White & Hajjar 1997, Surovek & White 2004, Tong & Xing 2007), little discussions can be found on the application of the notional load approach to a column subjected to gravity loads within its unsupported length, although Schmidt (2001) presented it for mill building columns. It is unclear to the engineer what the flexural effective length is for the bottom segment, or any of the upper segments, even when he or she uses the notional load approach or the equivalent horizontal forces. What is the "actual unsupported length" in this case? There is a belief that the use of an effective length factor equal to unity for the critical segment is unconservative, since there are no horizontal members connecting the column at each loaded point to adjacent columns. This belief appears to be justified by Clause 9.4.3 of the European drive-in rack design code (ERF 2012), which specifies that only the base and the top of the upright (column) are to be laterally restrained in the buckling model used to determine the effective length when "direct second-order analysis" method is carried out.

It will be explained and demonstrated in this paper that whether there is a horizontal member restraining the point of gravity loading or not is irrelevant to the flexural effective length to be used in the stability design check of the segment. For drive-in racks, the buckling model used to determine the flexural effective length is also independent of the horizontal restraints provided by the friction between the pallet bases and the pallet runners (Gilbert et al. 2014).

This paper aims to elucidate the implications of the equivalent horizontal forces, and explain the more economical procedure for determining the (elastic) flexural effective length of a column subjected to concentrated gravity loads within its unsupported length. The proposed buckling model can be applied to the design of drive-in rack uprights and mill building columns, where automated creation of buckling models with no manual efforts from the program user has been implemented for several years (Dematic 2009).

As this paper is only concerned with the flexural effective length of a column in a 2D second-order elastic analysis based design procedure, three-dimensional phenomena such as torsional warping and flexural-torsional buckling (Teh et al. 2004) are not discussed. Based on second-order plastic-zone analysis results, and making use of column curves, the proposed buckling model will be compared against the use of the unity effective length factor and the buckling model prescribed in Clause 9.4.3 of the European drive-in rack design code (ERF 2012).

2. How a compact steel column fails

A compact steel column does not reach its ultimate load-carrying capacity when it buckles elastically, but only fails when the critical cross-section has yielded sufficiently under combined compression and bending. Figure 2 shows that a column that has buckled elastically is able to sustain increased loading beyond the elastic buckling load P_e (Gere & Timoshenko 1991).

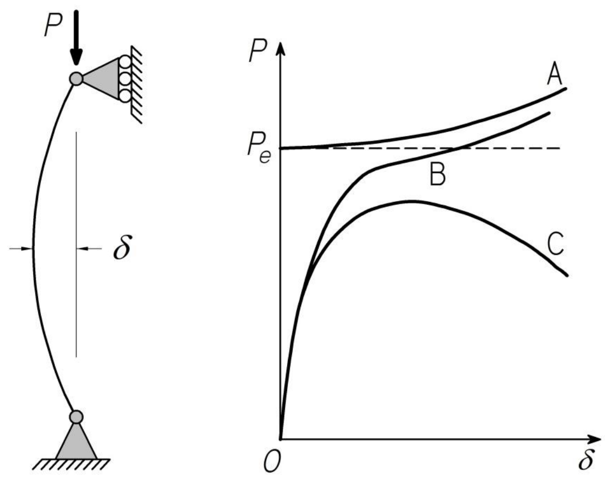

Figure 2 Behaviour and strength of a compact steel column (Gere & Timoshenko 1991)

Curve A in the figure denotes the load-deflection path of an elastic, perfectly straight column following its bifurcation. Curve B denotes that of an elastic, initially crooked column. The softening response exhibited by this curve is due to the P-δ effect. In each of the two cases, the column can always sustain increased loading since its resistance increases with increasing deformations to the extent that it equilibrates the quasi-statically applied load.

However, in reality, a compact steel column that buckles elastically would soon reach its ultimate load-carrying capacity as it encounters member instability due to (partial) yielding of the critical cross-section under combined compression and bending. For a simply supported column such as that shown in Figure 2, the bending moment at mid-span (the critical cross-section) results from the so-called P-δ effect. At the ultimate limit state, any further increase in the bending resistance of the mid-span due to increasing deformation could only match the increase in the P-δ effect if the applied load P decreases (while the displacement δ increases disproportionately).

Real steel columns invariably have initial crookedness, so a steel column typically follows the path denoted by Curve C in Figure 2. In any case, the ultimate load capacity of a column of a given section depends largely on its effective length L_e. The cantilevered and simply supported columns in Figure 3 have essentially the same ultimate load if they are composed of the same section. Based on this premise, column curves are used in steel structures design standards (SA 1998, AISC 2010, SA/SNZ 2005), where these curves may be represented by mathematical functions. The member compression capacity of an initially crooked column is determined from its effective length and the relevant column curve, which is typically derived for the simply supported condition (for which the effective length factor is unity).

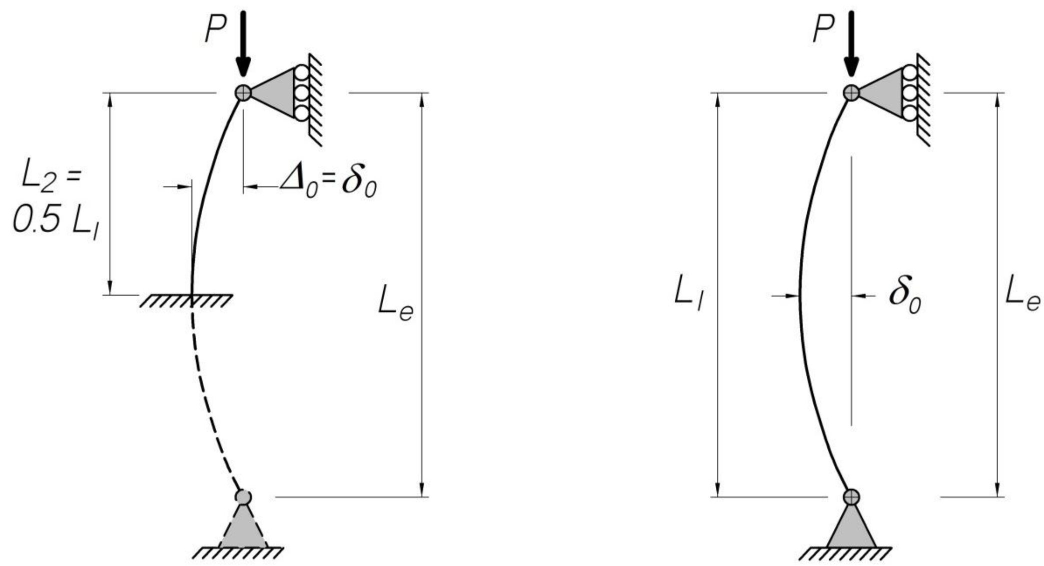

(a) (b)

Figure 3 Two equivalent columns

3. Implication of the equivalent horizontal forces

As illustrated in Figure 1, the equivalent horizontal forces prescribed in steel design standards (AISC 2010, ECS 2009, ERF 2012, RMI 2012, SA 1998) model the frame's nominal initial out-of-plumb. It has also been established by Liew et al. (1994) and Clarke & Bridge (1995) that, in a second-order analysis, the bending moments in the columns resulting from the application of the equivalent horizontal forces are virtually equal to those due to the initial out-of-plumb.

As discussed previously, the ultimate load P_u of an axially loaded cantilevered column such as that shown in Figure 3(a) can be determined directly from the relevant column curve and its effective length, which is twice its actual length, i.e. $P_u = P_c(L_e = 2L_2)$. Viewed as an equivalent simply supported column having a length twice its actual length, shown in Figure 3(b), no interaction equation between axial force and bending moment needs to be considered in determining its ultimate load capacity.

The free body, axial force and bending moment diagrams of the cantilevered column at the ultimate limit state, the latter two drawn for the assumed straight configuration, are shown in Figure 4. The bending moment M_u at the column base, which is due to the P-Δ effect, can be "reasonably" found through a second-order elastic analysis where the initial out-of-plumb Δ_0 of the cantilevered column is modelled, either explicitly or via an equivalent horizontal force. Viewed in this manner, it is clear that the column fails by the interaction between the axial force and the bending moment, and its capacity can be determined using the appropriate interaction equation. For bi-symmetric I-sections, and rectangular and square hollow sections that are compact, AS 4100 (SA 1998) specifies the following interaction equation where the ultimate moment M_u is given as

$$M_u = M_s\left\{\left[1-\left(\frac{1+\beta_m}{2}\right)^3\right]\left(1-\frac{P_u}{P_c'}\right)+1.18\left(\frac{1+\beta_m}{2}\right)^3\sqrt{\left(1-\frac{P_u}{P_c'}\right)}\right\} \qquad (1)$$

in which M_s is the section moment capacity, and β_m is the ratio of the smaller to the larger end moment, taken as positive when the column is bent in double curvature. The compression capacity P_c' is discussed in the next paragraph. Interested readers may consult Bridge & Trahair (1987) and Trahair & Bradford (1998) for the derivation and application of the design equation.

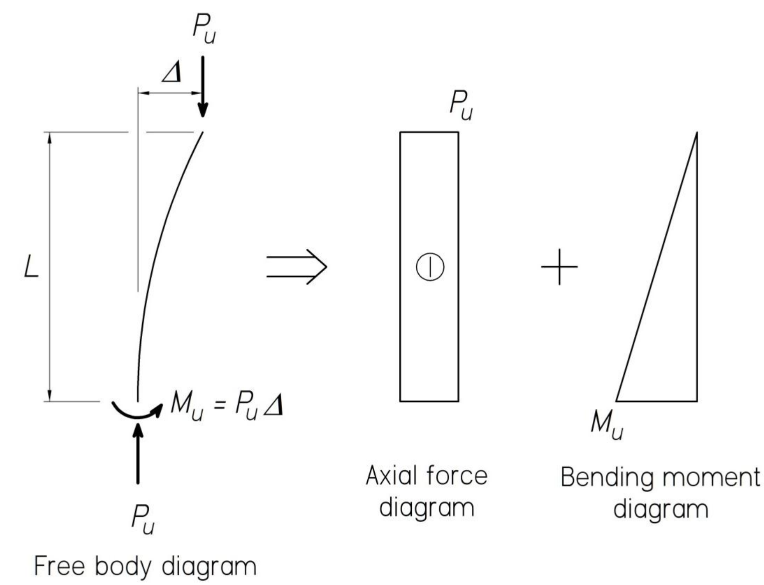

Figure 4 Force diagrams of a cantilevered column at the ultimate limit state

It can be seen that, for the cantilevered column, the compression capacity P_c' in Equation (1) must be greater than the ultimate load $P_u = P_c(L_e = 2L_2)$. In fact, the structural steel design standards (AISC 2010, SA 1998) specify that the compression capacity P_c' to be used in the interaction equation is equal to $P_c(L_e = L_2)$, i.e. the effective length factor is unity whether the member is braced or unbraced at both ends.

The preceding paragraph should resolve the doubt among drive-in rack designers whether an effective length factor equal to unity can be safely applied to the bottom segment of an upright when equivalent horizontal forces are included in the second-order analysis. In fact, as will be demonstrated later in this paper, the use of an effective length factor equal to unity in the interaction equation can be quite conservative in certain cases. The more correct procedure for determining the flexural effective length of a column segment is to apply a "notional" horizontal restraint where an equivalent horizontal force has been applied, in the buckling model. Figure 5(b) depicts the buckling model for the cantilevered column, which would result in an elastic effective length factor close to 0.7 (equal to 0.699 in three significant figures).

The notional horizontal restraint should be imposed onto the buckling model since the interaction equation is used to check the second-order bending moment resulting from the P-Δ effect. In other words, the destabilising effect due to the absence of a lateral restraint has been represented in the second-order analysis, and should not be duplicated in the buckling model to determine the effective length and therefore compression capacity P_c' in Equation (1). However, the implication of amplifying the bending moments due to the initial out-of-plumb (or equivalent horizontal forces) is less well appreciated in the literature, as reflected in the buckling model prescribed or allowed by certain standards (ERF 2012).

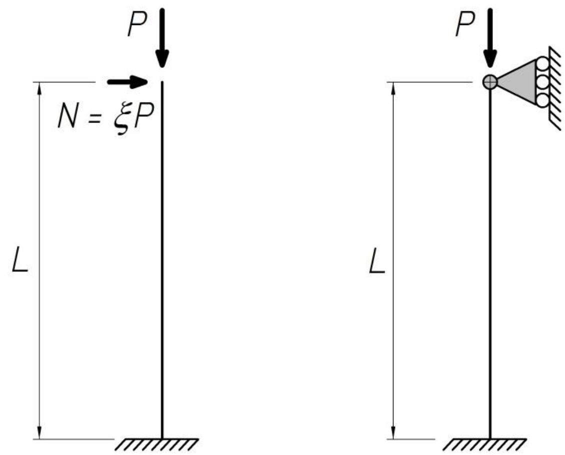

(a) (b)

Figure 5 Problem 4.1

As far as computer analysis programs such as RAD (Dematic 2009) are concerned, a notional horizontal restraint can be automatically imposed onto the buckling model at any node where an equivalent horizontal force has been applied in the second-order elastic analysis. For simplicity, and without sacrificing accuracy for practical structures, the notional horizontal restraints of a prismatic column subjected to more than one concentrated gravity load within its unsupported length can be applied simultaneously in a single buckling model for all the segments. It should be noted that, in practice, the critical segment of such a column is invariably the bottom one.

In addition to the member stability check represented by Equation (1), AS 4100 (SA 1998) requires that the member is checked against cross-section strength, which, for a compact rectangular or square hollow section, is represented by

$$M_u = 1.18 M_s \left(1 - \frac{P_u}{P_y}\right) \tag{2}$$

in which P_y is the squash load. However, as mentioned earlier, the cross-section strength check only governs stocky columns and those bent in substantial double curvature.

4. Verification problems

The column models analysed in this paper had an initial out-of-plumb $\xi = 0.002$ in both the second-order plastic and elastic analyses unless noted otherwise. However, no initial crookedness was modelled in the second-order elastic analyses as per the standard practice, while an initial crookedness δ_0 of $L/1000$ was invariably modelled in the plastic-zone analyses, the direct results of which are taken to be the correct ones.

In the following discussions, Method A refers to the use of the unity effective length factor to determine the compression capacity P_c' to be entered into Equation (1), and Method B refers to the use of the present buckling model, in which notional horizontal restraints are imposed where the equivalent horizontal forces have been applied.

The third method, called Method C, uses the buckling model described in Clause 9.4.3 of FEM 10.2.07 (ERF 2012). The buckling model is only relevant to the columns subjected to intermediate gravity loads within its unsupported length, and is shown in the following sub-sections where applicable.

Having determined the effective length of a column or column segment using either of the three aforementioned methods, the compression capacity P_c' to be entered into Equation (1) is read from the column curve shown in Figure 6. This curve has been derived through a series of plastic-zone analyses of simply supported columns having lengths ranging from 100 mm to 18,000 mm. Each of these columns was assumed to have an initial crookedness δ_0 of $L/1000$.

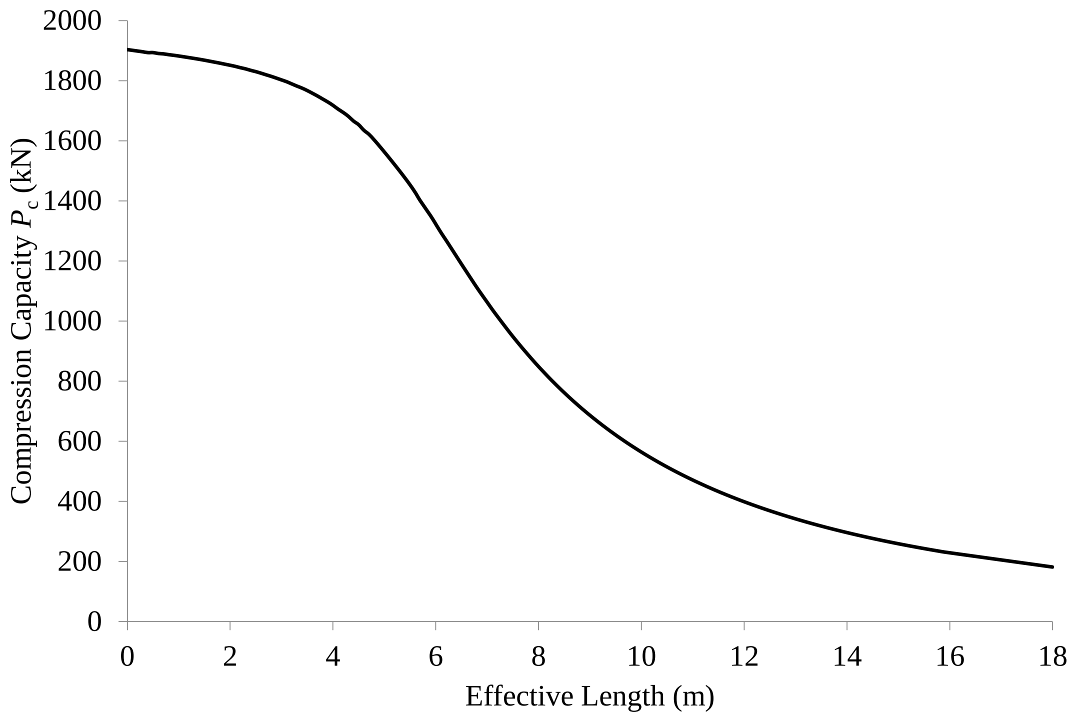

Figure 6 Column curve of SHS 203 × 6.3 (without residual stresses and strain hardening)

All the columns are composed of square hollow section (SHS) 203 × 6.3. This section was selected for three reasons. First, the issues of local, distortional, minor/major axis and flexural-torsional buckling are irrelevant to the square hollow section, ensuring proper evaluations of the alternative methods used to determine the flexural effective length. Second, an interaction equation that accounts for the bending moment gradient, namely Equation (1), is available for a square hollow section, enabling a more rigorous comparison of the various buckling models considered in this paper. Third, simply supported columns of various lengths composed of this section had been tested and analysed by Key & Hancock (1993), who provided the finite strip analysis results including that neglecting residual stresses. The finite element models used in the present plastic-zone analyses (Strand7 2010) could therefore be verified and employed with confidence.

The square hollow section has an area of 4,818 mm^2 and a second moment of area equal to 3.06 × 10^7 mm^4. The slenderness ratios L/r in the following problems range from 37 to 113.

For the purpose of this paper, the square hollow section was assumed to have a uniform yield stress of 395 MPa, which is the same as the flange yield stress in the analytical model of Key & Hancock (1993). No residual stresses nor strain hardening was assumed.

4.1 Cantilevered columns axially loaded at the top

This simple structure, depicted in Figure 5(a), is included in this paper to demonstrate that Equation (1) is not unduly conservative. This aspect is important since, in the following subsections, it will be asserted that the use of an effective length factor equal to unity (Method A), and the buckling model described in Clause 9.4.3 of FEM 10.2.07 (ERF 2012) that is used in Method C, lead to significant conservatism in the design of certain columns.

For a cantilevered column, both the elastic and the inelastic effective length factors are equal to 2. The buckling model used to determine the effective lengths in the present method (Method B) is depicted in Figure 5(b), which results in an elastic effective length factor equal to 0.7.

Table 1 lists the professional factors P_{ua}/P_{ud} of Methods A and B for 3000, 6000 and 9000 mm long columns. The variable P_{ua} denotes the ultimate load obtained by the second-order plastic-zone analysis, and P_{ud} is the ultimate load capacity determined through second-order elastic analysis in conjunction with Equations (1) and (2), which depends on the effective length used to read P_c' from the column curve shown in Figure 6.

Table 1: Results for cantilevered columns with $\xi = 0.002$

Case	***L* (mm)**	**P_{ua} (kN)**	**Method A ($L_e = L$)**		**Method B ($L_e = 0.7\,L$)**	
			P_c' (kN)	**P_{ua}/P_{ud}**	**P_c' (kN)**	**P_{ua}/P_{ud}**
4.1.1	3000	1289	1802	0.94	1841	0.94
4.1.2	6000	394	1323	0.98	1689	0.98
4.1.3	9000	180	684	0.99	1238	0.99

It can be seen from Table 1 that, for a cantilevered column axially loaded at the top, significant differences in the assumed effective length factors do not lead to noticeably different ultimate load capacities P_{ud}. For the 3000-mm column, the compression capacity P_c' entered into Equation (1) for the unity effective length factor is only 2% lower than that for the effective length factor of 0.7. For the other two columns, the reasons are twofold. First, a given percentage difference in the compression capacities P_c' translate to a much smaller one in the available moment capacities M_u given by Equation (1). Second, in the proximity of the ultimate load P_u, the second-order bending moment increases much more rapidly than the applied load.

However, when either method is used, the ultimate load capacity P_{ua} of the 3000-mm column is overestimated by more than 5% (Case 4.1.1 in Table 1). The reason is that the second-order bending moment at the ultimate limit state, which is the result of the P-Δ effect, is underestimated by the second-order elastic analysis. The elastic displacement of the 3000-mm column is about 30% less than the inelastic displacement at the ultimate limit state, as evident in Figure 7. For each case shown in the figure, the elastic curve is somewhat stiffer than the inelastic one, which is plotted thicker, due to the neglect of initial crookedness in the former and, for Case 4.1.1, subsequent inelasticity in the latter.

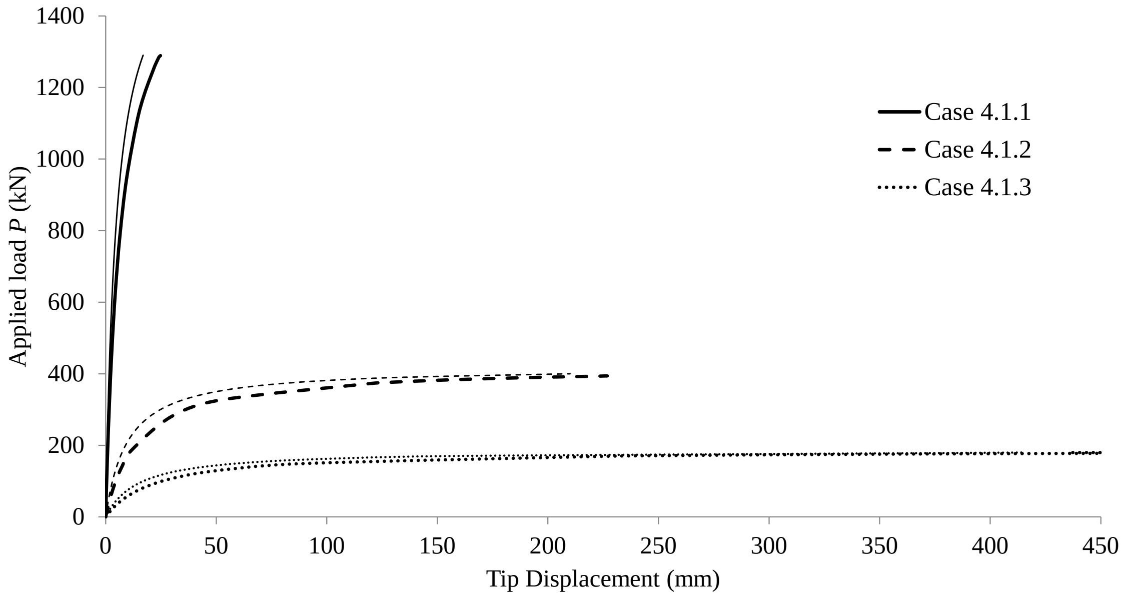

Figure 7 Elastic and inelastic load-deflection graphs of cantilevered columns

According to AS/NZS 4084 (SA 2012), the minimum initial out-of-plumb ξ is equal to 0.004 when second-order elastic analysis is performed, and 0.002 when second-order inelastic analysis is used. Table 2 shows the professional factors of Methods A and B when $\xi = 0.004$ is used in the second-order elastic analysis.

Table 2: Results for cantilevered columns with $\xi = 0.004$ in the elastic analysis

L (mm)	**P_{ua} (kN)**	**Method A ($L_e = L$)**		**Method B ($L_e = 0.7\,L$)**	
		P_c' (kN)	**P_{ua}/P_{ud}**	**P_c' (kN)**	**P_{ua}/P_{ud}**
3000	1289	1802	1.05	1841	1.04
6000	394	1323	1.02	1689	1.01
9000	180	684	1.01	1238	1.01

Tables 1 and 2 demonstrate that the use of Equations (1) and (2) in the second-order elastic analysis does not lead to undue conservatism for the SHS columns analysed in the present work. This finding means that the two equations are unlikely to be the source of any significant conservatism found in the following examples.

4.2 Columns with fixed bases and elastic restraints at the loading point

The example depicted in Figure 8(a) is interesting in that it demonstrates the conservatism of the unity effective length factor approach (Method A) in a certain case where the actual elastic effective length factor of the column is 1.0. Method B uses the buckling model depicted in Figure 8(b).

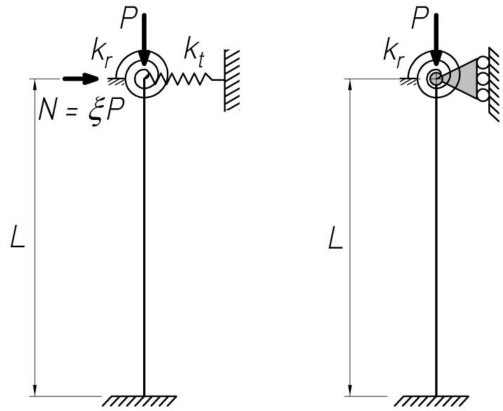

(a) (b)

Figure 8 Problem 4.2

This example also illustrates the consequence of using the same initial out-of-plumb in the second-order plastic and elastic analyses, which does not vary monotonically with the column slenderness. Another feature is that, except for Cases 4.2.2 and 4.2.3 listed in Table 3, the cross-section strength represented by Equation (2) governs when the proposed method (Method B) is used to determine the compression capacity P_c' to be entered into Equation (1).

Table 3: Results for columns with fixed bases and elastic restraints at the loading point

Case	***L* (mm)**	***K_t'***	***K_r'***	***P_{ua}* (kN)**	**Method A ($L_e = L$)**		**Method B (Fig. 11b)**	
					P_c' (kN)	**P_{ua}/P_{ud}**	**P_c' (kN)**	**P_{ua}/P_{ud}**
4.2.1	5000	1	1	1633	1560	1.06	1807	0.97 (0.93)
4.2.2		3	1	1777		1.14		0.99
4.2.3		3	3	1778		1.14	1817	0.98
4.2.4	7500	1	1	1022	949	1.12	1680	1.01 (0.99)
4.2.5		3	1	1384		1.46		0.95 (0.93)
4.2.6		3	3	1438		1.52	1720	0.95 (0.91)

Note: If the cross-section strength governs, the professional factor resulting from Equation (1) is given in brackets.

The normalised translational spring stiffness K_t' in Table 3 and subsequent tables is defined as

$$K_t' = \frac{k_t L^3}{3EI} \qquad (3)$$

in which E is the column's elastic modulus and I is its second moment of area. Therefore, a value of $K_t' = 1.0$ implies that the cantilevered column is translationally restrained by another identical (unloaded) column that is connected at the top via a pin-ended link.

The normalised rotational spring stiffness K_r' is defined as

$$K_r' = \frac{k_r L}{6EI} \tag{4}$$

An empty cell in Table 3 means that it has the same value as the above cell. This convention applies to all tables in this paper.

Table 3 shows that, even for Case 4.2.4, where the actual elastic effective length factor is equal to 1.0, the use of the unity effective length factor leads to some conservatism. The conservatism quickly escalates as the translational restraint increases. Note that the columns ($\xi = 0.002$) sway rather significantly under axial compression alone, as evident from the load-deflection graphs plotted in Figure 9.

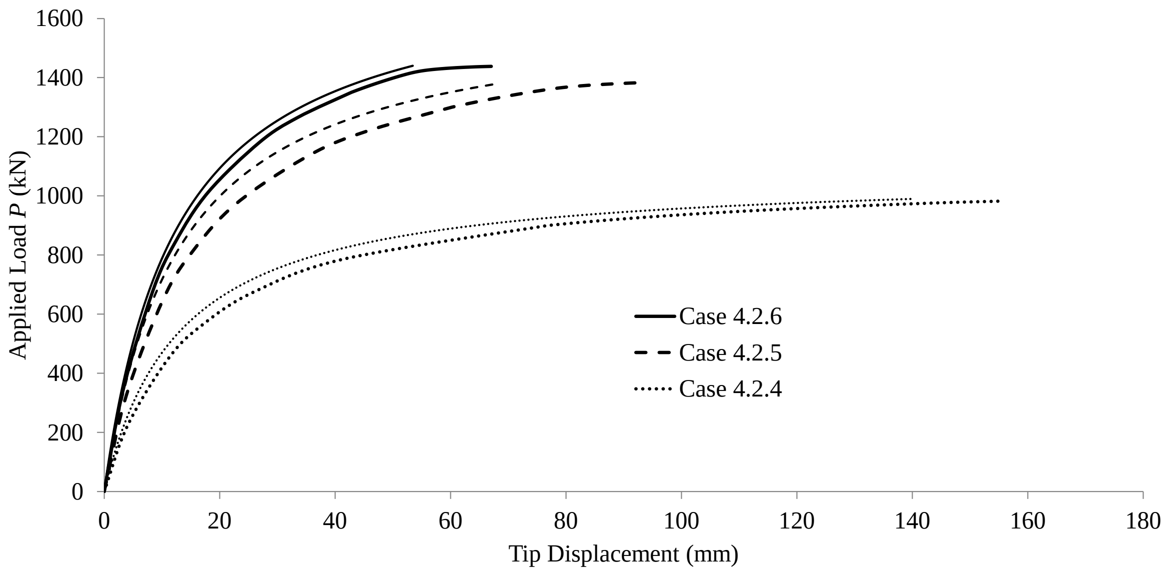

Figure 9 Elastic and inelastic load-deflection graphs of 7500-mm columns

It can be seen from Table 3 that, even when the same initial out-of-plumb $\xi = 0.002$ is used in both the second-order plastic and elastic analyses, the use of the proposed buckling model depicted in Figure 8(b) in conjunction with Equations (1) and (2) does not lead to over-optimistic capacities by more than 5%. This outcome is despite the 27% underestimation of the tip displacement at the ultimate limit state (and therefore the P-Δ effect) of Case 4.2.5 by the second-order elastic analysis, as evident in Figure 9. For each case shown in the figure, the elastic curve is noticeably stiffer than the inelastic one, which is plotted thicker.

4.3 Columns with one intermediate gravity load

The example depicted in Figure 10(a) has a loading arrangement that may be encountered in mill building columns (see also Problem 4.6), and shows cases where Methods A and C are alternately over-conservative while Method B, which uses the buckling model depicted in Figure 10(b), is consistently accurate. The buckling model used by Method C, described in Clause 9.4.3 of FEM 10.2.07 (ERF 2012), is shown in Figure 10(c). The "actual unsupported length" in Method A is the loaded length L_b.

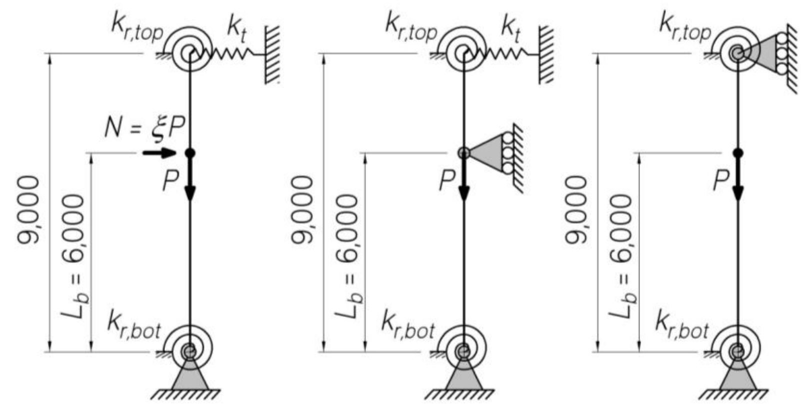

Figure 10 Problem 4.3

Table 4 shows that, for the pin-ended column (Case 4.3.1), the buckling model described in Clause 9.4.3 of FEM 10.2.07 (ERF 2012) and used in Method C leads to an underestimation of the ultimate load capacity by almost 20%. For the column with elastic rotational restraints (Case 4.3.2), the use of the unity effective length factor underestimates same by more than 30%. On the other hand, Method B is consistently accurate for both columns.

Table 4: Results for columns with one intermediate gravity load

Case	$K_r'{}_{bot}$	$K_t'{}_{top}$	$K_r'{}_{top}$	P_{ua} (kN)	Method A		Method B		Method C	
					P_c' (kN)	P_{ua}/P_{ud}	P_c' (kN)	P_{ua}/P_{ud}	P_c' (kN)	P_{ua}/P_{ud}
4.3.1	0	∞	0	1203	1324	1.07	1600	1.02	1098	1.18
4.3.2	1	∞	1	1765		1.33	1721	1.03	1624	1.09

4.4 Columns with two equally spaced gravity loads

The example depicted in Figure 11(a) has a loading arrangement that may be encountered in drive-in racks. The three methods of determining the effective length are compared across three different restraint conditions at the bottom and the top. Method A invariably uses the length of each segment, 5000 mm, as the effective length. Method B uses the buckling model depicted in Figure 11(b), while Method C uses that in Figure 11(c).

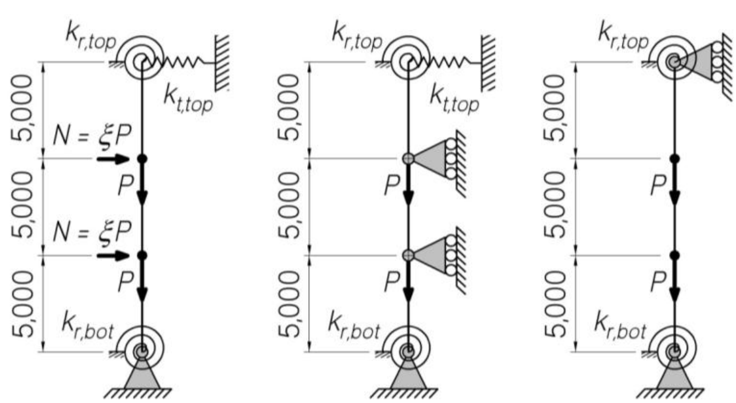

Figure 11 Problem 4.4

Table 5 shows that, for the first two columns, the three methods give the same results despite the differences in the compression capacity P_c' determined from the column curve. However, for the largest capacity column, Method C underestimates the ultimate load capacity by 15%.

Table 5: Results for columns with two equally spaced gravity loads

Case	$K_r'_{bot}$	$K_t'_{top}$	$K_r'_{top}$	P_{ua} (kN)	Method A		Method B		Method C	
					P_c' (kN)	P_{ua}/P_{ud}	P_c' (kN)	P_{ua}/P_{ud}	P_c' (kN)	P_{ua}/P_{ud}
4.4.1	1	1	1	400	1560	1.05	1716	1.05	996	1.05
4.4.2	∞	0	∞	484		1.03	1773	1.03	1389	1.03
4.4.3	1	∞	1	1092		1.00	1727	1.00	996	1.15

4.5 Columns with two unequally spaced gravity loads

The example depicted in Figure 12(a) has two unequally spaced gravity loads, and is interesting in that Method A determines the middle segment of the column without rotational restraint (Case 4.5.1 in Table 6) to be critical while Method B and C invariably determine the bottom segment to be critical for both cases shown in Table 6. For Case 4.5.1, Method C determines the effective length factor of the bottom segment to be 3.2. Method A uses each segment length as its effective length, Method B uses the buckling model depicted in Figure 12(b), and Method C uses that depicted in Figure 12(a) minus the horizontal loads.

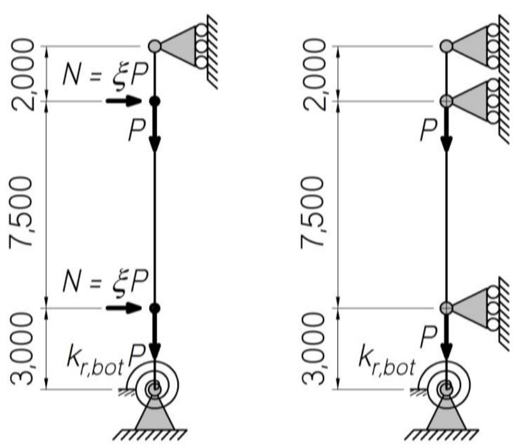

Figure 12 Problem 4.5

Table 6: Results for columns with two unequally spaced gravity loads

Case	$K_r'_{bot}$	P_{ua} (kN)	Method A		Method B		Method C	
			P_c' (kN)	P_{ua}/P_{ud}	P_c' (kN)	P_{ua}/P_{ud}	P_c' (kN)	P_{ua}/P_{ud}
4.5.1	0	630	949	0.99	1767	0.99	603	1.11
4.5.2	3	1394	1802	0.96	1781	0.96	1279	1.13

Although Methods A and B do not always determine the same segment to be critical, they yield essentially the same results that are accurate within 5%. On the other hand, Method C underestimates the ultimate load capacities by more than 10%.

4.6 Columns subjected to primary bending moments

All the preceding examples involve columns that are loaded concentrically, and are therefore subjected to secondary bending moments only due to the column's initial out-of-plumb and deflection (in addition to axial compression). The example depicted in Figure 13(a) is subjected to a primary bending moment due to a 200-mm eccentricity of the axial load *P*. Depending on the eccentricity direction, the primary bending moment may act clockwise or counter-clockwise.

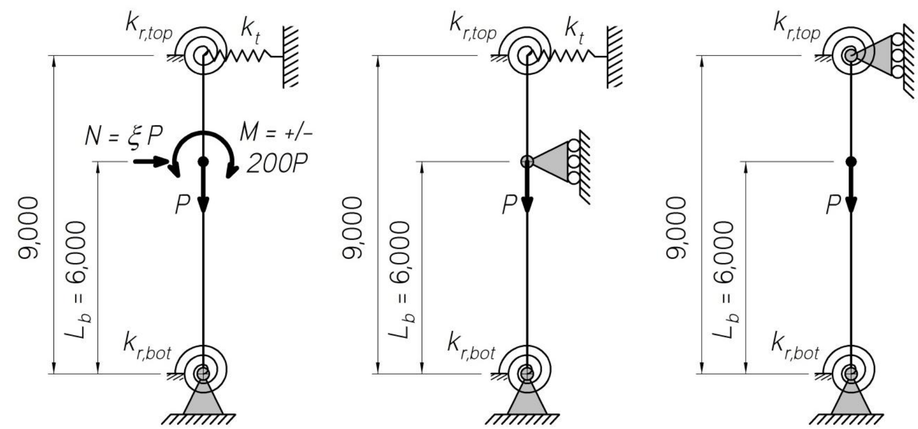

(a) (b) (c)

Figure 13 Problem 4.6

The "actual unsupported length" in Method A is the loaded length L_b. Method B uses the buckling model shown in Figure 13(b), while Method C uses that shown in Figure 13(c).

It can be seen from Tables 7 and 8 that, whether the primary bending moment acts in the clockwise or counter-clockwise direction, the proposed Method B is consistently accurate with errors less than 10%. In contrast, Methods A and C lead to errors of 15% or more in some cases.

Table 7: Results for columns subjected to a clockwise primary bending moment

Case	${K_r}'_{bot}$	${K_t}'_{top}$	${K_r}'_{top}$	P_{ua} (kN)	Method A		Method B		Method C	
					P_c' (kN)	P_{ua}/P_{ud}	P_c' (kN)	P_{ua}/P_{ud}	P_c' (kN)	P_{ua}/P_{ud}
4.6.1	0	∞	0	564	1324	1.02	1600	0.97	1098	1.09
4.6.2	1	∞	1	861		1.17	1721	1.04	1624	1.07

Table 8: Results for columns subjected to a counter-clockwise primary bending moment

Case	${K_r}'_{bot}$	${K_t}'_{top}$	${K_r}'_{top}$	P_{ua} (kN)	Method A		Method B		Method C	
					P_c' (kN)	P_{ua}/P_{ud}	P_c' (kN)	P_{ua}/P_{ud}	P_c' (kN)	P_{ua}/P_{ud}
4.6.3	0	∞	0	575	1324	1.08	1600	1.02	1098	1.15
4.6.4	1	∞	1	874		1.22	1721	1.09	1624	1.11

5. Summary and conclusions

The notional load approach, in conjunction with second-order elastic analysis, was conceived in order to allow the use of the "actual unsupported length" of a column in its stability design check. However, in structural engineering practice, it is unclear what the unsupported length is for a segment of a column with intermediate gravity loads where no lateral restraints exist. The European drive-in rack design code prescribes a buckling model that mostly results in effective length factors greater than unity. This paper points out that, in the context of second-order elastic analysis based design procedure, not only the effective length factor of a segment without lateral restraints at both ends needs not be greater than unity, it can even be significantly less than unity.

It is explained that, since the destabilising effect due to the absence of a lateral restraint has been represented in the second-order analysis that incorporates the notional horizontal load (or the equivalent horizontal force), a notional horizontal restraint should be imposed onto the buckling model in determining the effective length to be used in the interaction equation.

Based on the results of plastic-zone analysis incorporating an initial out-of-plumb equal to 0.002, it was found that, while the actual (inelastic) effective length factor of a cantilevered column is 2.0, the use of the braced effective length factor equal to 0.7 in conjunction with the second-order elastic analysis incorporating an initial out-of-plumb equal to 0.004 still led to a slightly conservative result. When an initial out-of-plumb equal to 0.002 was used in the elastic analysis, the braced effective length factor gave essentially the same results as the unity effective length factor, which are close to the plastic-zone analysis results.

It is demonstrated through twenty examples involving columns subjected to concentrated gravity loads within their unsupported lengths that the proposed buckling model can lead to designs that are more economical than the use of the unity effective length factor or the buckling model described in the European drive-in rack design code. Automatically imposing notional horizontal restraints onto the buckling model where equivalent horizontal forces have been applied in the second-order analysis can be implemented in a computer program without much difficulty, with potentially significant savings in the total cost of the drive-in racking system or mill building columns.

In this paper, for the sake of simplicity, all the notional horizontal restraints of a prismatic column subjected to more than one concentrated gravity load within its unsupported length are applied simultaneously to a single buckling model for all the column segments. This approach is reasonable for most practical columns including the uprights of a drive-in rack, where the design gravity loads and the spacings between them are largely uniform. The authors have analysed more than thirty columns having various end restraint and loading conditions, and have never found any case for which the proposed method leads to an unconservative error greater than 5%.

Acknowledgments
The authors would like to thank the Australian Research Council for supporting the second author through the Discovery Early Career Researcher Award (Project ID: DE140100212).

References

AISC (2010) "ANSI/AISC 360-10 Specification for Structural Steel Buildings." American Institute of Steel Construction.

ASCE (1997) "Effective Length and Notional Load Approaches for Assessing Frame Stability: Implications for American Steel Design." American Society of Civil Engineers.

Bridge, R.Q., Trahair, N.S. (1987) "Limit state design rules for steel beam-columns." *Steel Construction*, Australian Institute of Steel Construction, 21 (1) 2-11.

Clarke, M.J., Bridge, R.Q. (1995) "The notional load approach for the design of frames," *Research Report No. R718*, School of Civil and Mining Engineering, University of Sydney.

Dematic (2009) "Rack Analysis & Design (RAD) - User's Manual Version 6.9." Dematic Asia Pacific.

ECS (2009) "EN 15512 Steel static storage systems – Adjustable pallet racking systems." European Committee for Standardization.

ERF (2012) "FEM 10.2.07 The design of drive-in and drive-through racking." European Racking Federation.

Gere, J.M., Timoshenko, S.P. (1991) "Mechanics of Materials." Chapman & Hall.

Gilbert, B.P., Teh, L.H., Badet, R.X., Rasmussen, K.J.R. (2014) "Influence of pallets on the behaviour and design of steel drive-in racks." *Journal of Constructional Steel Research*, Elsevier, 97: 10-23.

Key, P.W., Hancock, G.J. (1993) "A theoretical investigation of the column behaviour of cold-formed square hollow sections." *Thin-Walled Structures*, Elsevier, 16 (1) 31-64.

Liew, J.Y., White, D.W., Chen, W.F. (1992) "Notional-load plastic-hinge method for frame design." *Journal of Structural Engineering*, American Society of Civil Engineers, 120 (5) 1434-1453.

RMI (2012) "ANSI/MH16.1 Specification for the design, testing and utilization of industrial steel storage racks." Rack Manufacturers Institute.

SA (1998). "AS4100 Steel Structures." Standards Australia.

SA (2012) "AS 4084 Steel storage racking." Standards Australia.

SA/SNZ (2005) "AS/NZS 4600 Cold-formed Steel Structures." Standards Australia.

Schmidt, J.A. (2001) "Design of mill building columns using notional loads." *Engineering Journal*, American Institute of Steel Construction, 38 (2) 90-99.

Strand7 (2010) "User manual - Release 2.4.4." G+D Computing Pty Ltd.

Surovek, A.E., White, D.W. (2004) "Alternative approaches for elastic analysis and design of steel frames." *Journal of Structural Engineering*, American Society of Civil Engineers, 130 (8) 1186-1205.

Teh, L.H., Gilbert, B P. (2016) "A buckling model for the stability design of steel columns with intermediate gravity loads." *Journal of Constructional Steel Research*, Elsevier, 117: 243-254.

Teh, L.H., Hancock, G.J., Clarke, M.J. (2004) "Analysis and design of double-sided high-rise steel pallet rack frames." *Journal of Structural Engineering*, American Society of Civil Engineers, 130 (7) 1011-1021.

Tong, G.S., Xing, G. (2007) "A comparative study of alternative approaches for stability design of steel frames." *Advances in Structural Engineering*, Multi-Science Publishing, 10 (4) 455-466.

Trahair, N.S., Bradford, M.A. (1998) "The behaviour and design of steel structures." E & FN Spon.

White, D.W., Clarke, M.J. (1997) "Design of beam-columns in steel frames." *Journal of Structural Engineering*, American Society of Civil Engineers, 123 (12) 1556-1575.

White, D.W., Hajjar, J.F. (1997) "Accuracy and simplicity of alternative procedures for stability design of steel frames." *Journal of Constructional Steel Research*, Elsevier, 42 (3) 209-261.